Istraživanja i projektovanja za privredu
ISSN 1451-4117
DOI:10.5937/jaes0-50819
www.engineeringscience.rs

iipp publishing

Journal of Applied Engineering Science
Vol. 22, No. 3, 2024
Original Scientific Paper
Paper number: 22(2024)3, 1228, 634-645

INFLUENCE OF EXHAUST FAN POSITION AND THE ADDITION OF SECONDARY EXHAUST FAN TO CONTROL INDOOR AIR POLLUTION (IAP) INSIDE A PARKING GARAGE

Pramadhony[1], Dewi Puspitasari[2], Muhammad Said[3], Kaprawi Sahim[2]*

[1] Universitas Tridinanti, Faculty of Engineering, Department Mechanical Engineering, Palembang, Indonesia
[2] Universitas Sriwijaya, Faculty of Engineering, Department Mechanical Engineering, Inderalaya, Indonesia
[3] Universitas Sriwijaya, Faculty of Engineering, Department Chemical Engineering, Inderalaya, Indonesia
** kaprawi@unsri.ac.id*

Air pollution has significantly deteriorated air quality in many urban areas, leading to numerous health issues. This pollution is not confined to outdoor environments but also affects indoor spaces, such as parking garages in basements. One major concern is cold-start emissions from idling cars, which produce higher concentrations of pollutants compared to normal hot emissions. Internal Combustion Engine Vehicles (ICEVs) emit cold-start emissions during the first few minutes after ignition. To mitigate this impact, parking operators typically use exhaust fans to replace polluted air with fresh air. However, the design and placement of the exhaust fan should be optimized to ensure a healthy indoor environment and efficient energy use. This research examines the concentration of air pollutants in a parking garage with three idling cars, focusing on the effectiveness of an exhaust fan installed in two different positions: near the parking spaces and near the pathway. Additionally, the research evaluates the impact of the exhaust fan's position and the inclusion of a secondary exhaust fan on carbon monoxide (CO) concentration during cold-start emissions. The results indicate that the primary exhaust fan should be installed in Position A, as it provides better airflow distribution and effectively extracts air pollutants. Improper airflow distribution, observed when the exhaust fan is installed in Position B, results in some measurement points showing high CO concentrations, with the highest average concentration reaching 68.9 ppm. Furthermore, the addition of a secondary exhaust fan helps reduce the average CO concentration and shortens the duration of the cold-start emission effect.

Keywords: indoor air quality, cold-start emission, emission dispersion, parking garage

1 INTRODUCTION

Urban air pollution has severely impacted human health, particularly affecting the respiratory system. In urban areas, air pollution primarily comes from various types of internal combustion engine vehicles (ICEVs) [1, 2]. This pollution affects both outdoors and indoors. This pollution affects both outdoor and indoor environments. However, research indicates that indoor environments have a more significant negative impact on human health than outdoor environments, as people tend to spend more time indoors. [3]. Several factors influence Indoor Air Pollution (IAP), including outdoor air quality, technologies for controlling indoor air pollution, and emission sources inside the room [4].

Basements used as parking garages require special attention due to the high concentrations of air pollutants from ICEV exhaust gases. The amount and concentration of pollutants inside a parking garage are strongly related to the number of cars present and the quality of the outdoor air [5, 6]. While outdoor air quality influences IAP, the primary focus should be on the emission sources, as they have a more significant impact on Indoor Air Quality (IAQ). Emission sources are particularly critical during cold-engine conditions, when CO concentrations can exceed 1%, much higher than under normal conditions [7]. Other important factors include the position of the emission sources and the flow characteristics of the exhaust gas [8]. Research also indicates that outdoor air quality affects the influx of fresh air into the parking garage and the activation time of the catalytic converter, which can significantly reduce pollutant concentrations [9, 10].

Air pollution dispersion is also influenced by the geometry of objects and the specifics of the exhaust fan. The shape and arrangement of objects inside the parking garage can alter the dispersion pattern of emissions and determine the locations of polluted areas [11]. Mechanical ventilation is essential for parking garages, as natural ventilation alone cannot provide a sufficient air change rate [12]. Improving air quality inside the garage can be achieved by adjusting the height of the exhaust fan or the direction of jet fans [13, 14].]. Exhaust fans play a crucial role in maintaining indoor air quality by replacing polluted air with fresh air. Additionally, the placement of the primary exhaust fan should consider the location of the emission source, as studies show that the highest concentrations of pollutants are found closest to the emission source [15].

Previously, air contaminants were removed after they had already polluted the indoor air. The concentration of air pollutants is governed by the emission rate and the efficiency of the mechanical ventilation system, as pollutants are released through the vehicle's exhaust. The authors suggest that removing air contaminants close to the emission source, specifically the tailpipe, can be effective. This objective can be achieved by incorporating an additional exhaust fan near the tailpipe, integrated with a set of "wheel stoppers," which are already mandated in parking garages.

Studying indoor air pollution using a full-scale model can be costly due to expensive tools and materials. To reduce costs, research can be conducted on a reduced-scale model, which lowers material expenses and allows for a controlled environment to assess the impact of various parameters [16]. The scale should account for the dimensions of the equipment and adhere to similarity factors [17].

In this research, experimental measurements are conducted on a reduced-scale model. Two exhaust fans are installed in the parking garage: the primary exhaust fan is mounted on the wall, while the secondary exhaust fan is positioned near the emission source and integrated into the wheel stopper. The research examines the influence of the secondary exhaust fan in controlling IAP and provides important information on the optimal positioning of the primary exhaust fan. Carbon monoxide (CO) concentration is chosen as a critical parameter for monitoring, as ICEVs emit this pollutant in high concentrations, especially during cold-start conditions [18].

2 MATERIAL AND METHOD

2.1 Materials of the parking garage

To investigate the impact of emissions inside a parking garage, the authors created a reduced-scale model with a scale of 1:8. The full-scale model measures 18 meters in length, 13 meters in width, and 3.5 meters in height. To enhance realism, four pillars are included to support the roof. The reduced-scale model is constructed using 2 x 4 cm Galvalume frames, aluminum composite panels, and 3 mm transparent acrylic panels. Holes are added to accommodate exhaust gas lines and the air sampler. Figure 1 illustrates the model sketch, while Table 1 compares the full-scale and reduced-scale models. Additionally, prototypes of cars resembling mini MPVs were created, each with a height, width, and length of 21.2 cm, 21.2 cm, and 50 cm, respectively. Each car model features a 6 mm diameter tailpipe as the emission source.

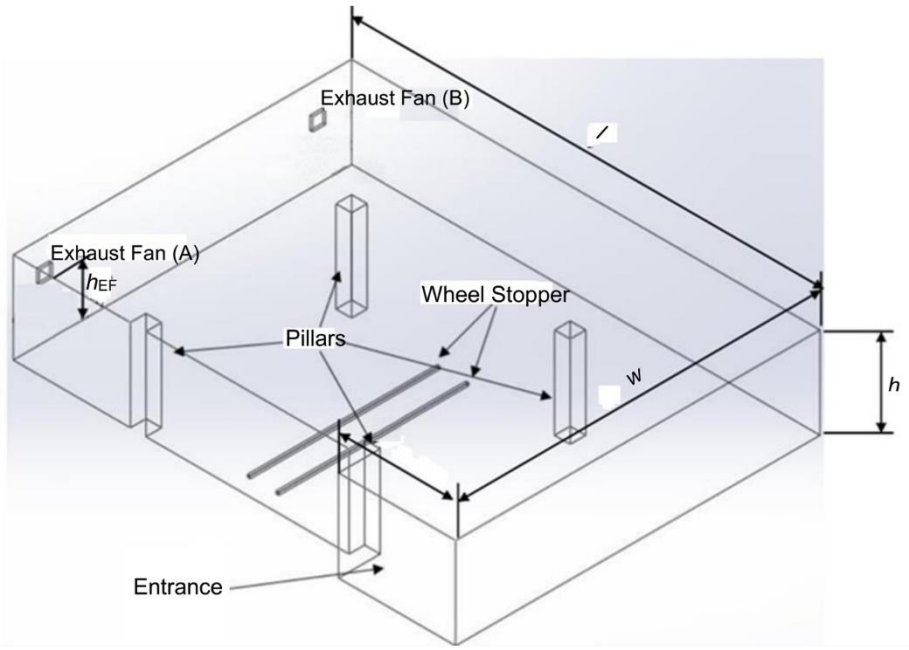

Fig. 1. Model of the parking garage

Table 1. Detailed dimensions of the full-scale and reduced-scale models

Symbol	Description	Dimension (cm)	
		Full-scale	Reduced-scale
l	Length of parking garage	1 800	225
w	Width of parking garage	1 300	162.5
h	Height of parking garage	350	43.75
$w_{air\ inlet}$	Width of air inlet	450	75
h_{ef}	Height of exhaust fan	250	31.25
w_{pillar}	Width of Pillar	60	7.5

2.2 Mass flow rate of ventilation

In the full-scale model, the exhaust fan provides air ventilation at a rate of three Air Changes per Hour (ACH). This ventilation rate is determined by the volume of the parking garage, as shown in Equation 1. When using the reduced-scale model, the volume rate must be adjusted to maintain dynamic similarity, ensuring that the Reynolds number remains consistent between the full-scale and reduced-scale models, as indicated in Equations 2 and 3.

$$Q_{air} = \frac{ACH \times A_{room} \times h_{room}}{3600} \quad (1)$$

where, Q_{air} = ventilation rate (m^3/s); ACH = air change per hour (h^{-1}); A_{room} =area of room (m^2); h_{room} = height of room (m).

$$Re_{Full-Scale} = Re_{Reduced-Scale} \quad (2)$$

$$Re = \frac{\rho u l}{\mu} \quad (3)$$

Where Re represents the Reynolds number; ρ (rho) is the fluid density; u is the fluid velocity; l is the characteristic linear dimension; and μ (mu) is the fluid viscosity. Using Equation 1, the full-scale model has an airflow rate of 0.68 m^3/s or 0.79 kg/s, assuming an air density of 1.16 kg/m^3. Applying this value to Equation 3, the ventilation rate for the reduced-scale model should be 0.0853 m^3/s or 0.0993 kg/s.

2.3 Rate of exhaust gas from cars

Three spark-ignition engine cars emit several hazardous air pollutants, particularly carbon monoxide (CO). This pollutant is primarily associated with cold-start emissions, which have much higher concentrations compared to hot emissions. This research uses actual exhaust gas taken from a car's tailpipe to obtain more reliable results [19]. During this period, Niraj Sharma and Ravi Sekhar Chalumuri observed that a spark-ignition engine car, while idling, consumes an average of 90 ml of fuel over 10 minutes [20]. This fuel consumption results in an exhaust gas mass rate of 1.793 g/s when the air-fuel ratio is set to 14.7. The exhaust gas is emitted by an M15A Suzuki engine with a 1.5-liter capacity, which meets the Euro-2 emission standard. For the reduced-scale model, Equation 4 is used to determine the exhaust gas rate. This equation ensures that the lambda (λ) ratio at full scale and reduced scale remains equal, where lambda (λ) is the ratio of the exhaust gas rate to the fresh air supply rate. Since the same fluid is used in the research as in actual conditions, Equation 5 follows a similar method, using air velocity as an indicator to determine the emission rate [21],[22].

$$\lambda_{at\ Full-Scale} = \lambda_{at\ Reduced-Scale} \quad (4)$$

$$\frac{\dot{m}_{EG\ at\ Full-Scale}}{\dot{m}_{air\ at\ Full-Scale}} = \frac{\dot{m}_{EG\ at\ reduced-scale}}{\dot{m}_{air\ at\ reduced-scale}} \quad (5)$$

This research assesses indoor air pollution during the cold-start emission phase. The exhaust gas passes through a reduced-scale tailpipe with a diameter of 6 mm, closely matching the typical full-scale tailpipe diameter of 1.9 inches, to produce a more realistic emission dispersion [23]. During this period, the concentration of CO remains constant for several minutes after starting the engine During this period, the concentration of CO remains constant for several minutes after starting the engine.

2.4 Variation of the model characteristic

This research examines the impact of exhaust fan positioning on indoor air quality. The primary exhaust fan is installed in two different locations: one near the parking area (Position A) and the other near the pathway (Position B). To assess the effects, three idling cars are positioned in two orientations: facing the exhaust fan and backing towards the exhaust fan. All cars are parked using reverse parking. Figure 2 illustrates the variations in the model configurations

After determining the optimal position for the primary exhaust fan, the research then examines the impact of the secondary exhaust fan. To manage energy consumption, the combined airflow rate of the primary and secondary exhaust fans should remain at the previous level (0.0853 m^3/s). In this setup, the primary exhaust fan's airflow rate is reduced to 85% of the total air change rate (0.0725 m^3/s), while the secondary exhaust fan contributes 15% of the total air change rate (0.0128 m^3/s). Figure 3 details the dimensions of the secondary exhaust fan (full scale) and the positioning of each hole relative to the cars' tailpipes inside the parking garage. The hole positions are designed to be as close as possible to the emission source (tailpipe). Additionally, the performance of the secondary exhaust fan has been previously evaluated through steady-state CFD modelling [24].

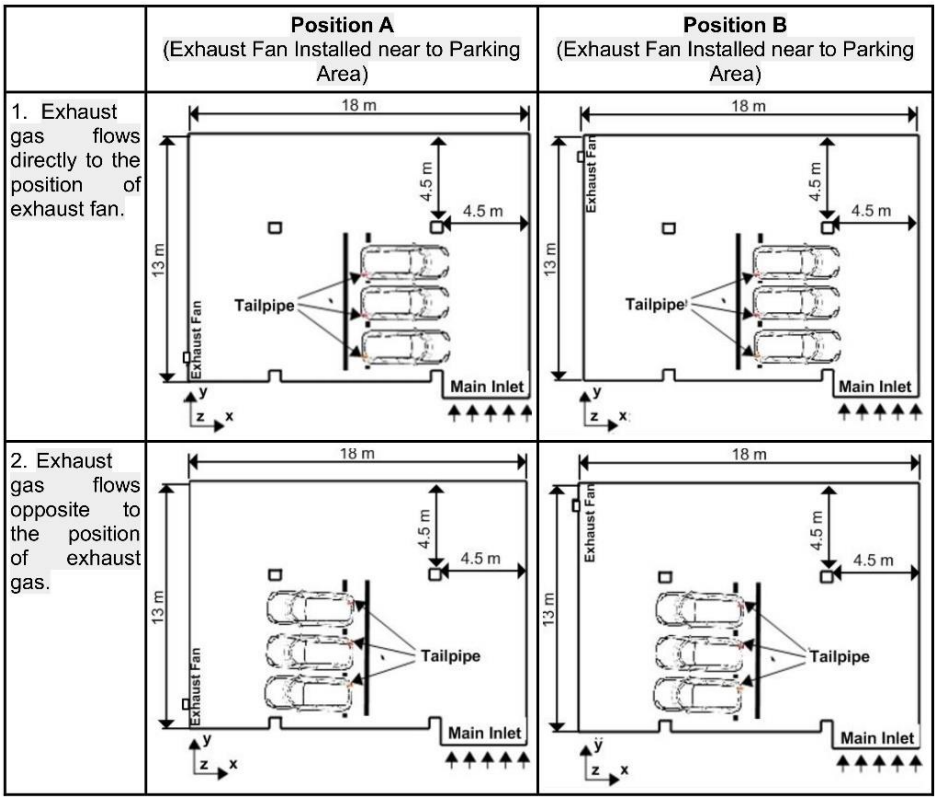

Fig. 2. Variations of the model characteristic

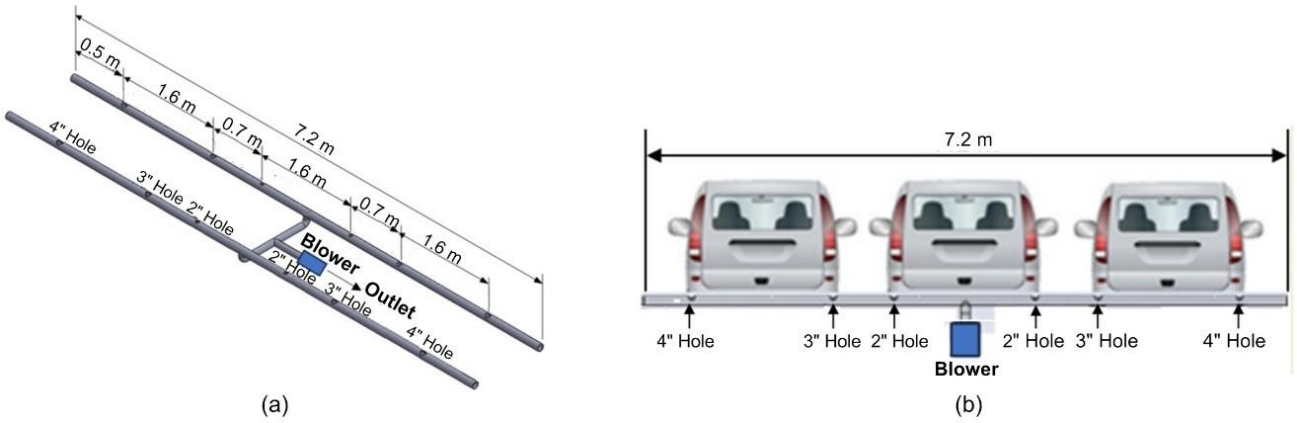

Fig. 3. Secondary exhaust fan (wheel stopper) (a) Detail dimension (b) Relative hole positions to cars inside parking garage

2.5 Experimental setup

This research employs two fluid flow systems: one for airflow ventilation and another for exhaust gas supply as the emission source. Two 600-watt electric blowers create airflow ventilation by removing air from inside the building, achieving a total flow rate of 0.171 m³/s or 614.25 m³/h. The flow rate is measured at a 4-inch pipe using a Lutron AM-4204HA hotwire anemometer, which has an accuracy of ±5%, following the US EPA guidelines for measuring emission flow rates. Additionally, a compressor draws exhaust gas from the tailpipe of a cold-start engine and distributes it to the tailpipe of a car prototype inside the parking garage. Each flow rate is regulated by three flow meters, each with a maximum capacity of 25 l/min. Fig. 4 illustrates the process of exhaust gas flowing from the cars' tailpipes to the car prototypes.

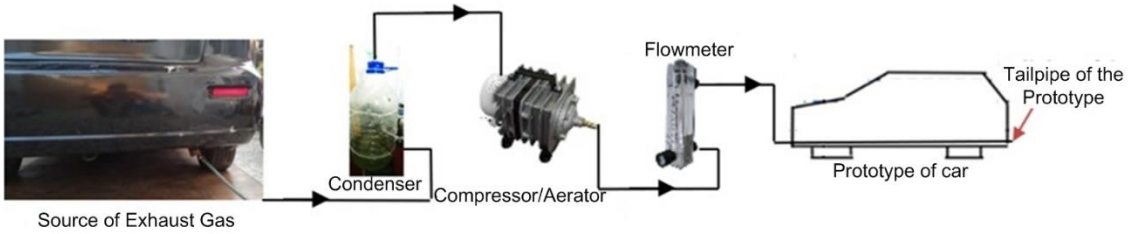

Fig. 4 Exhaust gas flows from the tailpipe of car to tailpipe of the prototype

To investigate emission dispersion from a cold engine, the process begins by activating the electrical blower to start air ventilation. Simultaneously, the compressor is turned on to inject exhaust gas from the tailpipe while the engine remains off. Additionally, a set of CO concentration measurement devices, including a sampling pump and gas detector, must be activated and prepared for recording pollutant concentrations. Once all mechanical equipment and measurement devices are functioning correctly, the engine is started, and CO concentration measurements are recorded. Fig. 5 illustrates the experimental setup used in the research.

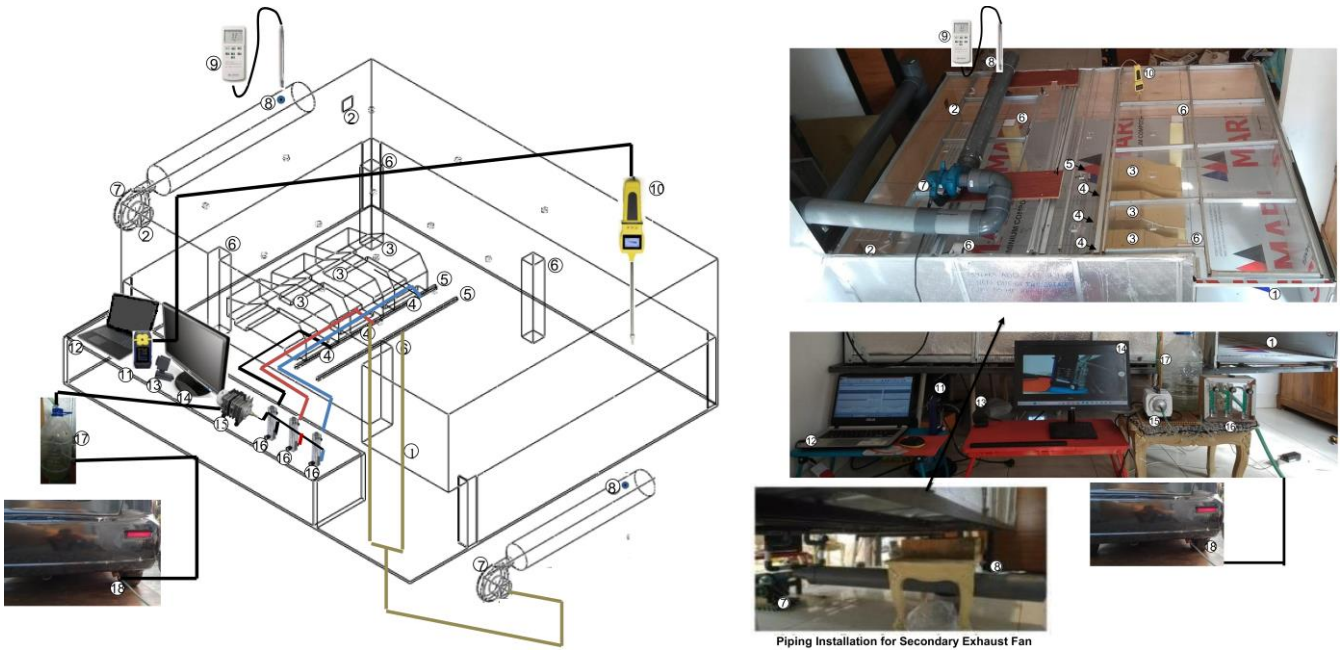

(a) (b)

Remark:

1. Inlet of Parking Garage
2. Outlet of Parking Garage
3. Cars
4. Tailpipe
5. Wheel Stoppers
6. Pillars
7. Electric Blower
8. Measurement Point of Air Velocity
9. Hotwire Anemometer
10. Air Sampler of Gas Detector
11. Gas Detector
12. Computer to Input Data
13. Webcam to Record Data of CO Concentration
14. Monitor to Display CO Concentration
15. Compressor to Inject Exhaust Gas
16. Flow Meter to Adjust Flow Rate of Exhaust Gas
17. Condenser to Separate Water from Exhaust Gas
18. Tailpipe as Emission Source

Fig. 5. Experimental Setup (a) Layout of the experimental setup (b) Photo of the experimental setup

2.6 Procedure of Measurement

A gas detector measures CO concentration, which is related to health issues. Measurements are taken at an adult breathing level (z-axis) of 1.5 meters m [25], [26], as depicted in Figure 7. The Bosean BH-4S multi-gas detector is used to analyze CO levels, with air samples collected using the gas sampling pump included in the package. This gas detector can measure CO concentrations ranging from 5 to 1000 ppm with an accuracy of ±5%. The CO concentration measurement process is illustrated in Fig. 6.

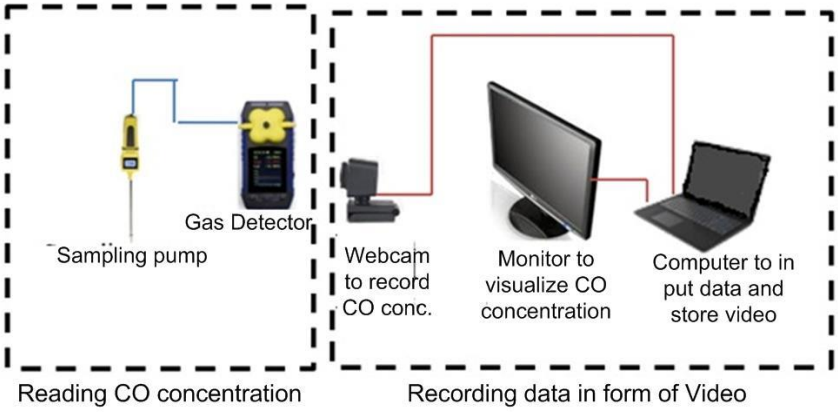

Fig. 6. Process of measuring CO concentration and recording the data

The prototype has fifteen measurement points: six in the pathway (PW) and nine in the parking area (PA). These points are created by drilling 13 mm diameter holes at specified locations on the prototype's cover, as shown in Figure 8. However, each case includes only twelve measurements, as each case features three cars, each assigned three measurement points. Consequently, the A-1 and B-1 cases do not have measurements at PA_3, PA_6, and PA_9. Conversely, the A-2 and B-2 cases lack measurements at PA_1, PA_4, and PA_7.

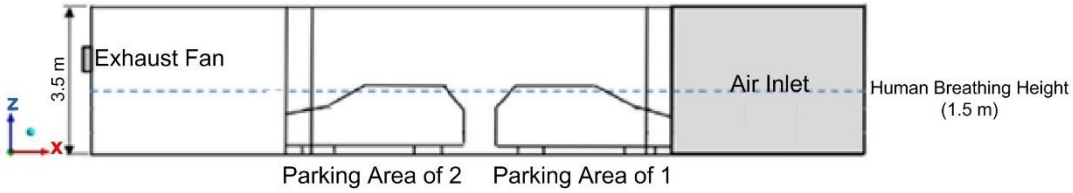

Fig. 7. Description of breath level

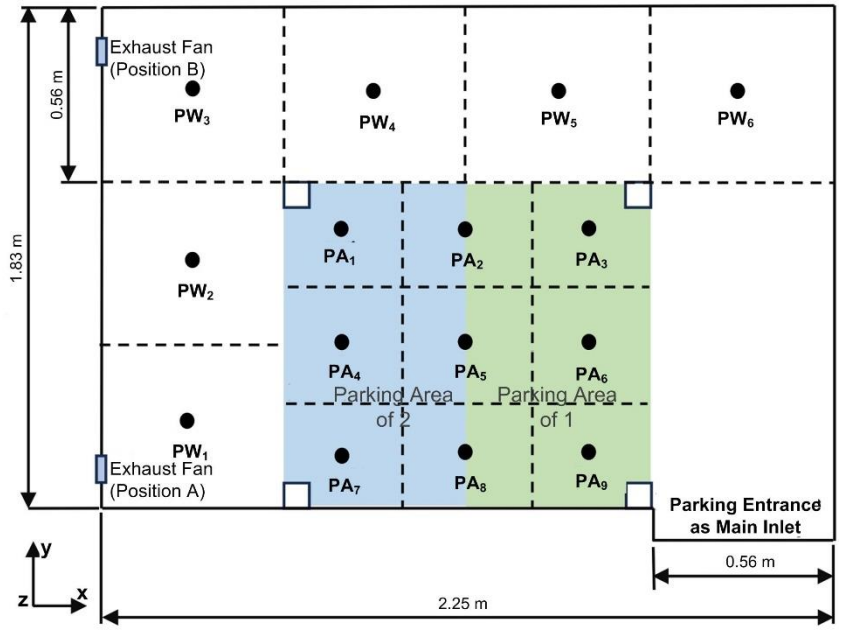

Fig. 8. Measurement points for measurement of CO concentration

3 RESULT AND DISCUSSION

3.1 Influence position of primary exhaust fan

Each model involves 12 CO concentration measurements at designated points, resulting in a total of 48 measurements. Each CO measurement lasts for ten minutes. CO concentrations are recorded 10 seconds after engine start and continue to be recorded at 30-second intervals. Consequently, completing all the measurements takes several days. Additionally, analysis of the emission source (exhaust gas) shows a CO concentration of 565 ppm. Measurements start when the engine temperature is low, as indicated by the Multi-Information Display (MID). The initial engine temperature was assessed by measuring the coolant temperature in the radiator using a TP 101 digital thermometer, which can measure temperatures ranging from -50 to 300 ºC with an accuracy of ±1 ºC. However, the engine is turned on when the temperature is already below 40°C to evaluate the effects of cold-start emissions.

After all measurements are completed, the CO concentration inside the parking garage is calculated to estimate the average CO concentration. The initial engine coolant temperature and the average CO concentration inside the parking garage are presented in Table 2. The results show that the CO concentration during the initial minutes of measurement significantly influences the average CO levels, confirming the high pollutant concentration during cold-start emissions. Figure 9, Figure 10, Figure 11, and Figure 12 illustrate the CO concentration trends over time at each measurement point for cases A-1, A-2, B-1, and B-2, respectively. These figures also compare the CO concentrations to the environmental threshold (which should be below 100 mg/m³ or 87 ppm), highlighting their potential health impact [27]. Generally, the figures demonstrate that cold-start emissions lead to increased CO concentrations at some measurement points during the first five minutes, but these levels gradually decrease as the CO concentration from the emission source diminishes

Figures 9 and 10 display the CO concentration trends for cases A-1 and A-2, where the exhaust fan is positioned near the parking area or emission source. Each figure is divided into two graphs: the left side (a) illustrates the impact at the parking area, while the right side (b) shows the impact at the pathway inside the parking garage.

Comparing the two exhaust fan positions, Case A-2 has a greater impact than Case A-1. In Case A-1, where the cars are positioned in Parking Area 1, the exhaust gas flows in the same direction as the airflow. In contrast, in Case

A-2, with cars situated in Parking Area 2, the exhaust gas flows opposite to the airflow, leading to wider dispersion of the exhaust gas into the surrounding area.

The highest CO concentration peak was observed in Case A-1. In this scenario, the exhaust gas was less dispersed, resulting in higher CO concentration at PW_1, where most of the exhaust gas is directed towards the primary exhaust fan. Although Case A-1 experienced the highest CO concentration peak, Case A-2 had a higher average CO concentration, especially at measurement point PA_6. The peak CO concentration in Case A-1 at PW_1 is due to the exhaust gas being concentrated in that area by the airflow, which only briefly impacts CO levels. Conversely, Case A-2, with its highest average CO concentration at PA_6, demonstrates a different issue. This point, near the parking garage's inlet but not directly aligned with the airflow direction, experiences reduced fresh air flow, leading to higher CO concentration.

Table 2. The initial engine coolant temperature and the average CO concentration inside the parking garage due to cold-start emission

Measurement Point	Initial engine coolant temperature (ºC)				Average CO concentration (ppm)			
	Case A-1	Case A-2	Case B-1	CaseB-2	Case A-1	Case A-2	Case B-1	CaseB-2
PW_1	34,4	33,6	37,5	34,1	17.1	11.5	65.2	11.5
PW_2	34,5	32,5	30,7	35,3	<5	9.3	25.7	17.0
PW_3	33,3	32,0	37,3	35,0	<5	10,0	17.4	11.9
PW_4	35,0	36,1	32,4	35,3	<5	13.3	6.6	14.5
PW_5	32,9	37,9	37,3	31,6	<5	19.0	5.9	18.5
PW_6	33,8	34,3	34,7	32,3	<5	15.0	5.2	20.2
PA_1	32,3	-	34,9	-	<5	-	9.3	-
PA_2	34,8	31,2	31,9	38,9	<5	15.2	21.9	11.5
PA_3	-	34,7	-	31,5	-	11.4	-	13.7
PA_4	31,2	-	33,8	-	<5	-	44.4	-
PA_5	33,1	35,0	36,1	35,9	<5	11.3	29.5	12.1
PA_6	-	36,0	-	35,1	-	29.9	-	15.0
PA_7	35,8	--	35,2	-	7.3	-	68.9	-
PA_8	39,2	34,9	34,9	34,8	<5	16.7	61.6	14.0
PA_9	-	34,9	-	39,0	-	22.7	-	15.2

Remark: Not measured due to the placement of the car prototypes at the measurement points

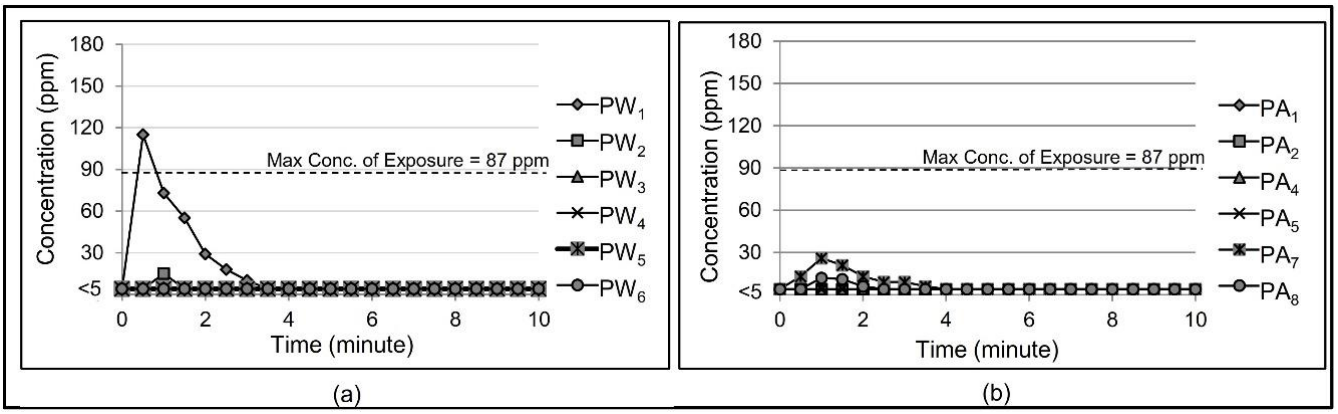

Fig. 9. Trends of CO concentration during cold-start emission for case of A-1 (Exhaust fan on Position A and cars are parked in the area of 1)

(a) in the pathway of parking garage (b) in the parking area of parking garage

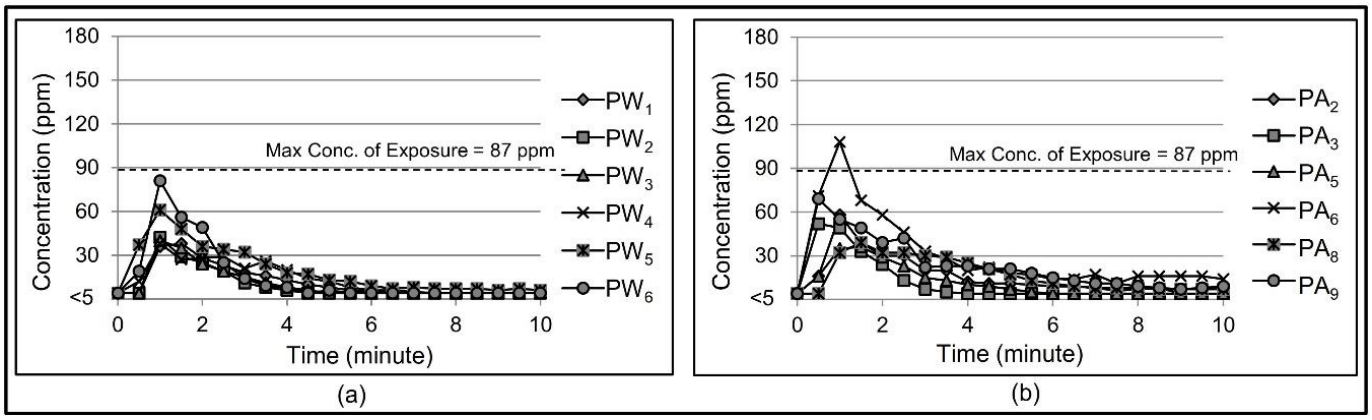

Fig. 10. Trends of CO concentration during cold-start emission for case of A-2 (Exhaust fan on Position A and cars are parked area of 2)

(a) In the pathway of parking garage (b) in the parking area of parking garage

Figures 11 and 12 illustrate CO concentration trends for cases B-1 and B-2, where the exhaust fan is positioned relatively far from the parking area. Similar to Figures 9 and 10, these figures are divided into two graphs: the left side (a) depicts the impact on the parking area, while the right side (b) shows the impact on the pathway.

In contrast to the exhaust fan positioned at Position B, cars parked in Parking Area 1 (Case B-1) have a greater impact than those in Case B-2, with the highest average CO concentration of 68.9 ppm at measurement point PA_7. This case has the most significant impact compared to others. Two main factors contribute to the elevated CO concentration in Case B-1 at certain points: insufficient fresh air and a greater volume of exhaust gas directed towards these points. In Case B-2, however, the exhaust gas flows against the airflow, which facilitates better mixing of exhaust gas and fresh air. As a result, the overall average CO concentration in Case A-2 and Case B-2 is quite similar, even though the CO levels at individual measurement points vary between the two cases.

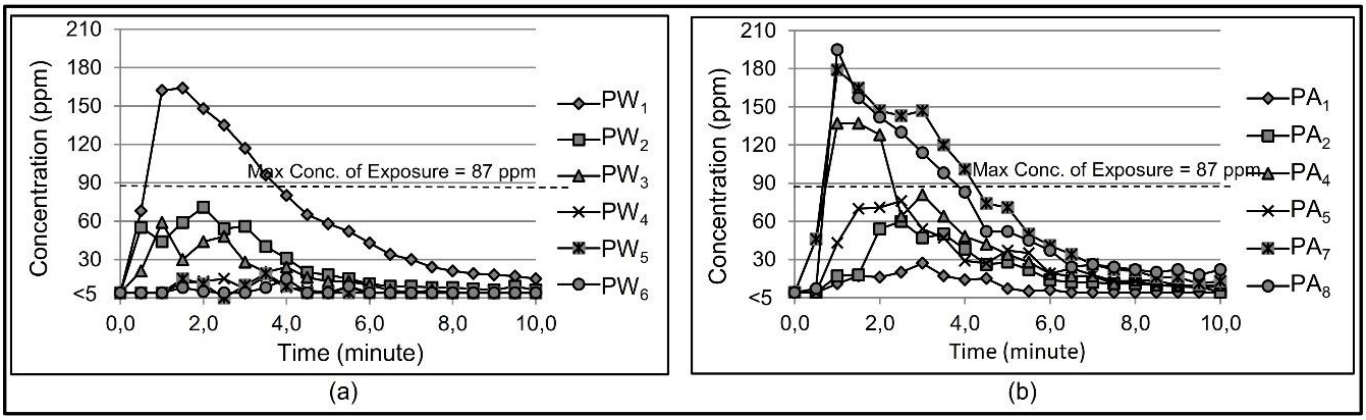

Fig. 11**.** Trends of CO concentration during cold-start emission for case of B-1 (Exhaust fan on Position A and cars are parked in the area of 1)

(a) In the pathway of parking garage (b) in the parking area of parking garage

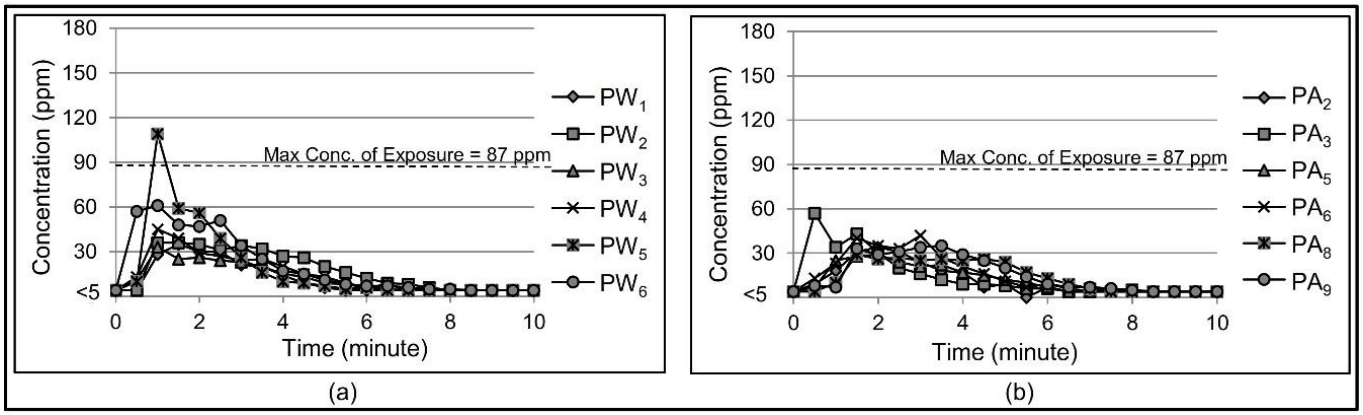

Fig. 12. Trends of CO concentration during cold-start emission for case of B-2 (Exhaust fan on Position A and cars are parked in the area of 2)

(a) In the pathway of parking garage (b) in the parking area of parking garage

In general, high CO concentrations at certain measurement points can be attributed to the proximity of exhaust gas flow to those points and their closeness to the emission sources. Additionally, insufficient fresh air supply around these measurement points also contributes to elevated CO levels [28], [29]. Vehicles parked and idling in Parking Area 2 have a broader impact on air pollution for both Case A-2 and Case B-2. In this position, the exhaust gas flows against the primary airflow direction, requiring more space for the exhaust gas to change direction, mix with fresh air, and eventually be removed by the exhaust fan.

When comparing the effectiveness of the exhaust fan positions, Position A proves to be more effective than Position B. The exhaust fan in Position A provides improved airflow distribution and minimizes dead zones. Consequently, this position results in better indoor air quality and lower CO concentrations, creating a healthier environment.

3.2 Influence the addition of secondary exhaust fan

After evaluating the effect of the primary exhaust fan position, it was found that Position A provides a larger healthy area. However, this position also leads to higher CO concentrations, especially in the parking area. To address this, a secondary exhaust fan integrated into the wheel stopper is proposed. This section of the research focuses on Case A-2, where the impact of idling cars in Parking Area 2 is greater than that in Parking Area 1. Table 4 compares the average CO concentrations with and without the secondary exhaust fan.

Overall, the secondary exhaust fan reduces the average CO concentration in the parking garage by 21.9%. According to Table 4, it effectively reduces the average CO levels at all measurement points in the pathway area (PW_1, PW_2, PW_3, PW_4, PW_5, PW_6). In the parking area, it reduces CO concentrations at three measurement points (PA_5, PA_8, PA_9), but increases them at PA_2, PA_3, and PA_6.

Figure 10 illustrates the CO concentration over a ten-minute period from engine start. Generally, the addition of a secondary exhaust fan raises the peak CO concentration, with the exceptions of measurement points PW5 and PW6, as shown in Figures 10 (e) and (f). The secondary exhaust fan creates a vacuum effect at certain holes or grills, drawing the exhaust gas away from these points and preventing contamination. Additionally, this secondary exhaust fan rapidly reduces CO concentrations to below 5 ppm.

Table 3. The average CO concentration inside the parking garage due to cold-start emissions under conditions without and with the secondary exhaust fan

Measurement Point	Initial Engine Coolant Temperature (ºC)		Average CO Concentration (ppm)	
	Without Secondary Exhaust Fan (SEF)	With Secondary Exhaust Fan (SEF)	Without Secondary Exhaust Fan (SEF)	With Secondary Exhaust Fan (SEF)
PW_1	33,6	34,40	11,5	8,3
PW_2	32,5	32,50	17,0	9,2
PW_3	32,0	35,30	11,9	9,3
PW_4	36,1	38,60	14,5	9,4
PW_5	37,9	37,80	18,5	10,3
PW_6	34,3	36,50	20,2	12,3
PA_2	31,2	38,20	11,5	11,9
PA_3	34,7	37,50	13,7	16,8
PA_5	35,0	36,50	12,1	11,4
PA_6	36,0	33,80	15,0	17,6
PA_8	34,9	34,70	14,0	8,6
PA_9	34,9	36,20	15,2	11,8
Average	-	-	14,6	11,4

Although the secondary exhaust fan results in higher peak CO concentrations at the nine measurement points, these elevated levels persist for a shorter duration. The secondary exhaust fan generates a vacuum that traps exhaust gases close to the parking area while effectively removing a significant amount of CO from the exhaust. Consequently, the CO concentration drops to below 5 ppm in an average of 4.3 minutes, significantly faster than the 7.1 minutes required without the secondary exhaust fan.

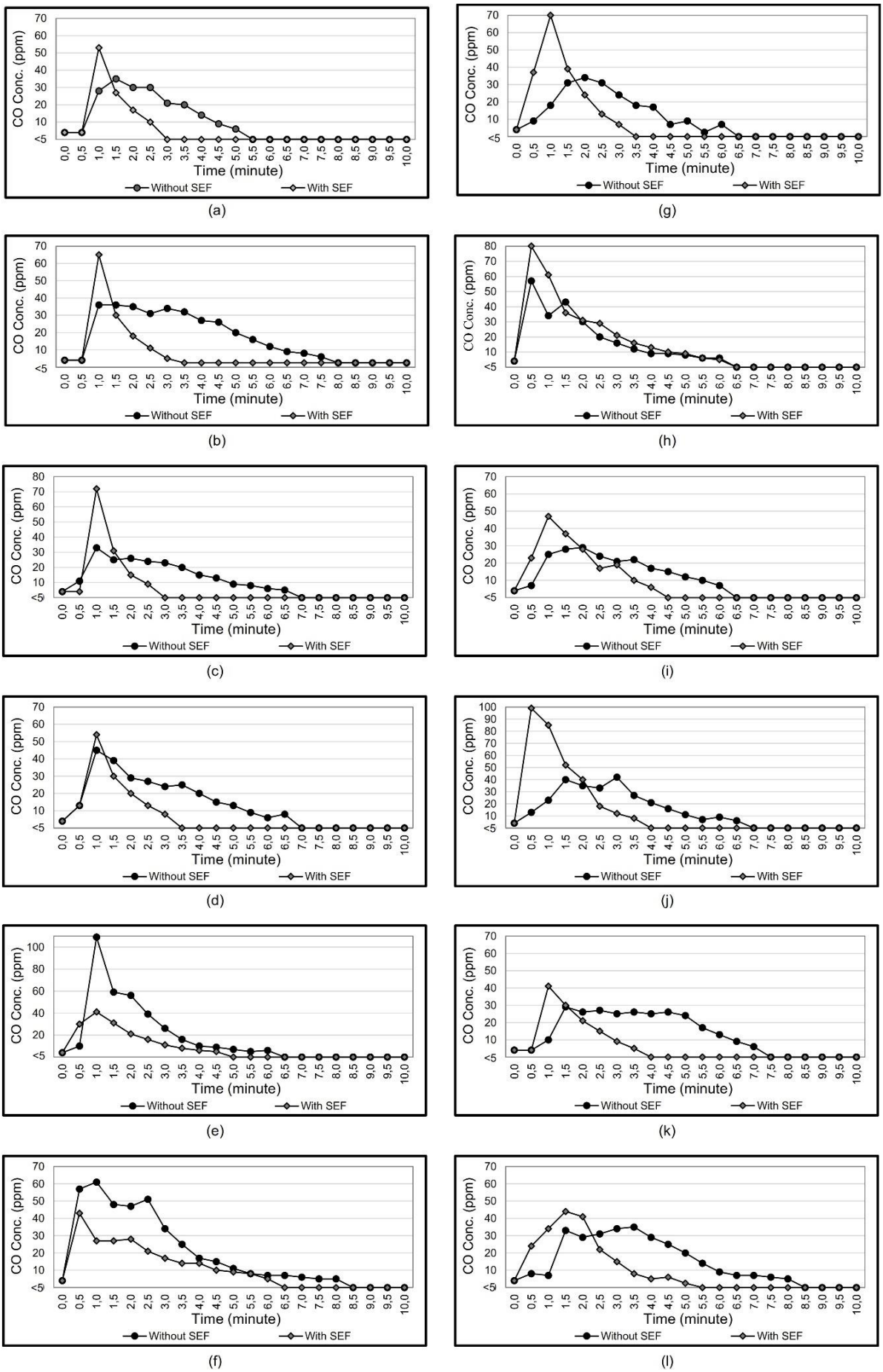

Fig. 13 Comparison of CO concentration trends with and without the Secondary Exhaust Fan (SEF) for measurement points: (a) PW1, (b) PW2, (c) PW3, (d) PW4, (e) PW5, (f) PW6, (g) PA2, (h) PA3, (i) PA5, (j) PA6, (k) PA8, (l) PA9

4 CONCLUSIONS

A 1:8 reduced-scale model of a parking garage was constructed to study the effects of cold-start emissions on indoor air quality (IAQ), specifically focusing on CO levels. The results showed that high CO concentrations from cold-idling vehicles significantly affect CO levels inside the garage. Generally, the highest CO concentrations occur within the first few minutes after the engine starts, after which the levels gradually decrease and stabilize at lower concentrations.

The worst conditions for CO levels are observed when vehicles are parked and idling in Position 2. In this position, the exhaust gas disperses extensively, resulting in greater air pollution inside the garage. However, this position also has the most significant impact, especially when the exhaust fan is located in Position B. In this case, the exhaust gas tends to accumulate in certain areas due to inadequate fresh air flow, referred to as dead zones. Conversely, the highest CO concentration occurs when cars are parked in Position 1, particularly in Case B-1, where the measurement point PA_7 records an average concentration of 68.9 ppm.

The measurements indicate that the primary exhaust fan performs best when installed in Position A, near the parking area. This setup enhances airflow distribution and reduces dead zones. On the other hand, placing the exhaust fan in Position B leads to larger dead zones due to insufficient fresh air flow. Consequently, CO levels in these dead zones remain high even after the engine is turned off, due to lower air velocity and limited air supply.

Relying solely on the primary exhaust fan requires a greater air supply, leading to higher energy use. Adding a secondary exhaust fan can help reduce indoor air pollution and cut down on energy consumption, especially during cold-start emissions. Although the secondary fan has a lower airflow rate, it efficiently captures air pollutants and prevents wider emission dispersion. While it may cause a rise in peak CO concentrations, it shortens the duration of the cold-start emission effect. Finally, the secondary exhaust fan reduces the average CO concentration inside the parking garage by 21.9%.

5 REFERENCES

[1] S. Sunarno, P., Purwanto, and B. Warsito. (2022). Analysis of Indonesia's Three Major Antropogenic Pollutants Which Include Various Emissions and Fuel Sectors in the 1990-2015 Period. Jurnal Pendidikan. IPA Indonesia. vol. 11, no. 2, 260–270, DOI: 10.15294/jpii.v11i2.33224.

[2] I., Sukarno, H., Matsumoto, and L., Susanti. (2016). Transportation energy consumption and emissions - a view from city of Indonesia. Future Cities Environment. vol. 2, no. 7, 1-23, DOI: 10.1186/s40984-016-0019-x.

[3] V., Van Tran, D., Park, and Y., C., Lee. (2020). Indoor air pollution, related human diseases, and recent trends in the control and improvement of indoor air quality. International Journal of Environmental Research and Public Health, vol. 17, no. 8, DOI: 10.3390/ijerph17082927.

[4] V., Vasile, V., Iordache, and V., M., Radu. (2023). The influence of ventilation on indoor air quality in buildings with variable pollutant emissions. IOP Conference Series: Earth and Environmental Science. vol. 1185, no. 1. DOI: 10.1088/1755-1315/1185/1/012006.

[5] A., Chaloulakou, A., Duci, and N., Spyrellis. (2002). Exposure to carbon monoxide in enclosed multi-level parking garages in the central Athens urban area. Indoor Built Environment. vol. 11, no. 4,191–201, DOI: 10.1159/000066017.

[6] F., Al-Rukaibi, N., Al-Mutairi, and A., Al-Rashed. (2018). Concentration of air pollutants in an urban parking garage in Kuwait. World Review of Science, Technology and Sust. Development. vol. 14, no. 2–3, 241–265, DOI: 10.1504/WRSTSD.2018.093217.

[7] J., Pielecha, K., Skobiej, and K., Kurtyka. (2021). Testing and evaluation of cold-start emissions from a gasoline engine in RDE test at two different ambient temperatures. Open Engineering. vol. 11, no. 1, 425–434, DOI: 10.1515/eng-2021-0047.

[8] M., Wu, G., Zhang, L., Wang, X., Liu, and Z., Wu. (2022). Influencing Factors on Airflow and Pollutant Dispersion around Buildings under the Combined Effect of Wind and Buoyancy—A Review. International Journal of Environmental Research and Public Health, vol. 19, no. 19, DOI: 10.3390/ijerph191912895.

[9] A., A., Melbert, Y., A., Shaposhnikov, A., V., Mashensky, and S., A., Voinash. (2019). Effects of 8Y12/12 catalytic converter prestarting on harmful emissions at negative ambient temperatures. IOP Conf. Series: Journal of Physics: Conf. Series. vol. 1177, no. 1, DOI: 10.1088/1742-6596/1177/1/012011.

[10] J., Gao, G., Tian, A., Sorniotti, A., E., Karci, and R., Di Palo. (2019). Review of thermal management of catalytic converters to decrease engine emissions during cold start and warm up. Applied Thermal Engineering. vol. 147, 177–187, DOI: 10.1016/j.applthermaleng.2018.10.037.

[11] S., Brusca, F., Famoso, R., Lanzafame, S., Mauro, M., Messina, and S., Strano. (2016). PM_{10} Dispersion Modeling by Means of CFD 3D and Eulerian-Lagrangian Models: Analysis and Comparison with Experiments. Energy Procedia, vol. 101, 329–336, DOI: 10.1016/j.egypro.2016.11.042.

[12] I., Suriaman, Mardiyati, J., Hendrarsakti, and A., D., Pasek. (2018). The improvement of indoor air quality (IAQ) by using natural and mechanical method. AIP Conference Proceding. vol. 1984, No. 1, DOI: 10.1063/1.5046602.

[13] J., Aminian, M., Maerefat, and G., Heidarinejad. (2018). The enhancement of pollutant removal in underground enclosed parking lots by reconsideration of the exhaust vent heights. Tunnelling and Underground Space Technology. vol. 77, 305–313, DOI: 10.1016/j.tust.2018.04.005.

[14] S., Ahn, H., Kwon, G., Kim, and J., Yang. (2016). Study of Securing Required Ventilation Rates and Improving Mechanical Ventilation Systems for Underground Parking Lots. Journal of Asian Architecture and Building Engineering. vol. 15, no. 3, 659–665, DOI: 10.3130/jaabe.15.659.

[15] E., Asimakopoulou, D., Kolaitis, and M., Founti. (2009). CO dispersion in a car-repair shop : An experimental and CFD modelling study. Seventh International Conference on CFD in the Minerals and Process Industries.

[16] Y., Tominaga and T., Stathopoulos. (2016). Ten questions concerning modeling of near-field pollutant dispersion in the built environment. Building Environment. vol. 105, 390–402, DOI: 10.1016/j.buildenv.2016.06.027.

[17] D., Prakash and P., Ravikumar. (2015). Analysis of thermal comfort and indoor air flow characteristics for a residential building room under generalized window opening position at the adjacent walls. International Journal of Sustainable Built Environment. vol. 4, no. 1, 42–57, DOI: 10.1016/j.ijsbe.2015.02.003.

[18] Y., Chang, B., Mendrea, J., Sterniak, and S., V., Bohac. (2017). Effect of Ambient Temperature and Humidity on Combustion and Emissions of a Spark-Assisted Compression Ignition Engine. Journal of Engineering for Gas Turbines and Power. vol. 139, no. 5, DOI: 10.1115/1.4034966.

[19] A., Moscatello et al. (2020). Scaling procedure for designing accidental gas release experiment. Engineering Computations. vol. 38, no. 3, pp. 1350–1367, DOI: 10.1108/EC-12-2019-0566.

[20] N., Sharma, R., Sekhar Chalumuri, A., Singh, and P., Kumar. (2017). Evaluation of Idling Fuel Consumption of Vehicles Across Different Cities. [Online]. Available: https://www.researchgate.net/publication/318788877_Evaluation_of_Idling_Fuel_Consumption_of_Vehicles_Across_Different_Cities

[21] C., K., Saha, G., Zhang, J., Q., Ni, and Z., Ye. (2011). Similarity criteria for estimating gas emission from scale models. Biosystems Engineering. vol. 108, no. 3, 227–236, DOI: 10.1016/j.biosystemseng.2010.12.005.

[22] R., J., Smith and P., J., Watts. (1994). Determination of Odour Emission Rates from Cattle Feedlots: Part 2, Evaluation of Two Wind Tunnels of Different Size. Journal of Agricultural Engineering Research, vol. 58, no. 4. 231–240, DOI: 10.1006/jaer.1994.1053.

[23] F., Liu, H., Qian, Z., Luo, S., Wang, and X., Zheng. (2020). A laboratory study of the expiratory airflow and particle dispersion in the stratified indoor environment. Building and Environment, vol. 180, DOI: 10.1016/j.buildenv.2020.106988.

[24] Pramadhony, K., Sahim, D., Puspitasari, M., Said, and Sugianto. (2023). The Integration of Exhaust Fan and Wheel Stopper to Reduce Indoor Air Pollution Inside the Enclosed Parking Garage. Proceedings of the 6th Mechanical Engineering, Science and Technology International conference (MEST 2022), 494-505, DOI: 10.2991/978-94-6463-134-0.

[25] A., Sharma and P., Kumar. (2020). Quantification of air pollution exposure to in-pram babies and mitigation strategies. Environment International. vol. 139, DOI: 10.1016/j.envint.2020.105671.

[26] A., B., Pulungan, M., Julia, J., R., Barubara, and M., Hermanussen. (2018). Indonesian National Synthetic Growth Charts. Acta Scientific Paediatrics. vol. 1, no. 1.

[27] World Health Organization, WHO global air quality guidelines. 2021, from https://www.who.int/publications/i/item/9789240034228, accessed on 2023-09-19.

[28] Pramadhony, K., Sahim, D., Puspitasari, M., Said, and Sugianto. (2023). The Effects of the Exhaust Fan Position to Indoor Air Pollution Distribution in Enclosed Parking Garage. CFD Letters. vol. 15, no. 3, 123–138, DOI: 10.37934/cfdl.15.3.123138.

[29] M., García-Díaz, C., Sierra, C., Miguel-González, and B., Pereiras. (2019). A discussion on the effective ventilation distance in dead-end tunnels. Energies, vol. 12, no. 17, DOI: 10.3390/en12173352.

Paper submitted: 03.05.2024.

Paper accepted: 12.08.2024.